598–606 *Nucleic Acids Research, 2008, Vol. 36, No. 2* *Published online 1 December 2007*
doi:10.1093/nar/gkm1077

Overlapping activator sequences determined for two oppositely oriented promoters in halophilic Archaea

Martina Bauer, Larissa Marschaus, Muriel Reuff, Verena Besche, Simone Sartorius-Neef and Felicitas Pfeifer*

Institut für Mikrobiologie und Genetik, TU Darmstadt, Schnittspahnstrasse 10, D-64287 Darmstadt, Germany

Received August 31, 2007; Revised and Accepted November 15, 2007

ABSTRACT

Transcription of the genomic region involved in gas vesicle formation in *Halobacterium salinarum* (p-vac) and *Haloferax mediterranei* (mc-vac) is driven by two divergent promoters, P_A and P_D, separated by only 35 nt. Both promoters are activated by the transcription activator GvpE which in the case of P_{mcA} requires a 20-nt sequence (UAS) consisting of two conserved 8-nt sequence portions located upstream of BRE. Here, we determined the two UAS elements in the promoter region of p-vac by scanning mutageneses using constructs containing P_{pD} (without P_{pA}) fused to the *bgaH* reporter gene encoding an enzyme with β-galactosidase activity, or the dual reporter construct pApD with P_{pD} fused to *bgaH* and P_{pA} to an altered version of *gvpA*. The two UAS elements found exhibited a similar extension and distance to BRE as previously determined for the UAS in P_{mcA}. Their distal 8-nt portions almost completely overlapped in the centre of P_{pD}–P_{pA}, and mutations in this region negatively affected the GvpE-mediated activation of both promoters. Any alteration of the distance between BRE and UAS resulted in the loss of the GvpE activation, as did a complete substitution of the proximal 8-nt portion, underlining that a close location of UAS and BRE was very important.

INTRODUCTION

The extremely halophilic *Halobacterium salinarum* and the moderately halophilic *Haloferax mediterranei* produce gas vesicles depending on environmental factors (1). We are interested in mechanisms of gene regulation in halophilic Archaea and use the *gvp* gene clusters encoding the proteins required for gas vesicle formation as model system. Gas vesicle formation involves the two gene clusters *gvpACNO* and *gvpDEFGHIJKLM*, which are oppositely oriented in the vac region (2). Two different vac regions of *H. salinarum* PHH1 are known, the plasmid pHH1-encoded p-vac and the chromosomal c-vac region, and in addition the chromosomal mc-vac region of *H. mediterranei*. The 14 *gvp* genes found in each of these vac regions encode slightly different variants of the two gas vesicle structural proteins GvpA and GvpC, and of additional Gvp proteins required for the assembly of this structure. GvpD and GvpE regulate the expression, with GvpE serving as transcriptional activator and GvpD being involved in the repression of gas vesicle formation (2–5). GvpD and GvpE are able to interact, and the interaction results in the breakdown of GvpE (4,6).

Transcription in Archaea is driven by a multi-subunit RNA polymerase (RNAP), and the initiation of basal transcription requires in addition to RNAP the TATA-box-binding protein TBP and the transcription factor TFB. A typical archaeal promoter consists of a TATA-box (= binding site of TBP) centred 24–28 nt upstream of the transcriptional start site, and the TFB-recognition element BRE located upstream and adjacent to the TATA-box (7,8). In all three vac-regions, the two promoters P_A and P_D are located upstream of the oppositely oriented *gvpA* and *gvpD* reading frames, and in the case of p-vac and mc-vac, the two BRE sequences are separated by 35 nt only (Figure 1A) (2). In contrast, the respective two promoters of c-vac are separated by 56 nt due to a 21-nt insertion upstream of P_{cD}–BRE. Except for P_{cD}, all of the P_A and P_D promoters are activated by GvpE (9–11). Besides studying the mRNAs by northern analysis in the original wild-type strains, these promoters have been analysed in *Haloferax volcanii* transformants using promoter fusions with *bgaH* as reporter gene encoding an enzyme with β-galactosidase activity (11–13). From the analyses of transformants containing the P_{mcA}- and P_{pA}–*bgaH* constructs it appears that cGvpE is the strongest activator followed by mcGvpE and pGvpE (11).

*To whom correspondence should be addressed. Tel: +06151 16 2957; Fax: +06151 16 2956; Email: pfeifer@bio.tu-darmstadt.de

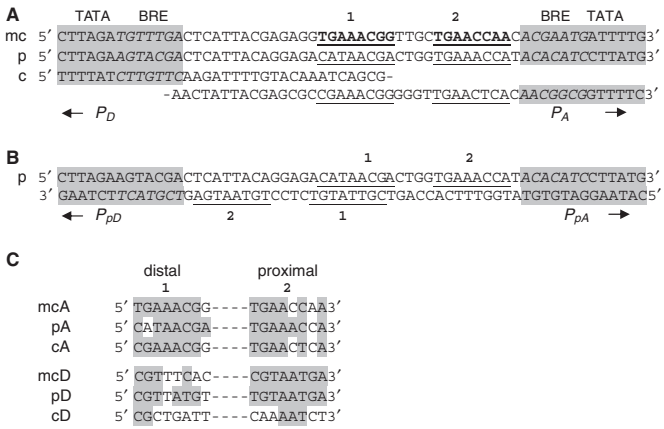

Figure 1. Comparison of the three intergenic regions between P_A and P_D in different vac-regions, and alignment of the 8-nt UAS portions. (**A**) The vac regions are designated mc (mc-vac), p (p-vac) and c (c-vac). The TATA-box and BRE elements (in italics) are shaded in grey. The sequence determined as GvpE-responsive element (UAS) in P_{mcA} is in bold and underlined, and the two conserved 8-nt portions are labelled 1 and 2. Related sequences in p-vac and c-vac are also underlined. (**B**) Divergent double-stranded P_{pA}–P_{pD} promoter sequence with the two putative UAS underlined. Arrows point to the direction of transcription. (**C**) Alignment of the 8-nt portions of the putative UAS elements found in the P_A and P_D promoters. The conserved sequences are shaded in grey. The distal (1) and the proximal (2) 8-nt portions of the UAS are indicated.

Two scanning mutageneses have been performed to determine the sequence elements required for the basal transcription and for the GvpE-mediated activation *in vivo*. The first series of 4-nt mutations encompassed a 50-nt region upstream of the transcription start site of p-*gvpA*, and the results of this study clearly define the TATA-box and BRE in P_{pA}, but also a region around position –10 that might serve as additional contact site of TFB (9,14). Mutations close to the 5′-end of this 50-nt sequence also affected the GvpE-mediated activation in P_{pA} (most strongly by altering the sequence AACCA upstream of BRE), but the mutations between the TATA-box and the start site of transcription had no effect on the GvpE-mediated activation (9).

The P_{mcA} promoter of mc-vac was used for the second 4-nt scanning mutagenesis encompassing the sequences upstream of the P_{mcA}-BRE, and this study defined the 20-nt sequence TGAAACGG-n4-TGAACCAA adjacent to BRE as important for the GvpE-mediated activation (Figure 1A) (13). A significant drop in the GvpE-induced activation is observed when two 8-nt portions of this element (labelled 1 and 2 in Figure 1) are mutated in steps of 4-nt, but a residual activity of 6–20% is still observed (BgaH activity quantified by ONPG assay). *In silico* analysis suggests similar 20-nt elements in all three P_A promoters and implies that they might serve as upstream activator sequence (UAS) for the GvpE-mediated activation (Figure 1A). The AACCA sequence mentioned above is part of the proximal 8-nt portion of this element in P_{pA}, and mutations up to CTGG had only a minor effect on the GvpE-induction in p-vac (9). Whether similar 20-nt UAS elements also occur in the GvpE-activated P_D promoters is not yet known and topic of the present report. *In silico* analysis indicated two similar elements in P_{mcD} and P_{pD} (Figure 1C). If a similar 20-nt UAS is found for P_D, the two divergent UAS in the P_D–P_A promoter region must overlap considerably in the centre of the 35-nt of intervening sequence as shown for p-vac in Figure 1B.

In this report, we analysed the P_{pD}–P_{pA} promoter region by 5-nt scanning mutagenesis to determine the respective UAS element required for the GvpE-mediated activation of both promoters in *H. volcanii* transformants. Using pGvpE, cGvpE or mcGvpE to activate P_{pD}-*bgaH* again defined cGvpE as strongest activator protein. A 5-nt scanning mutagenesis performed with P_{pD}–*bgaH* clearly yielded an UAS element of similar size as determined in the previous P_{mcA}-study. The effect of mutations was also analysed in the dual reporter construct $pApD_{UGA}$ (containing 3 UGA stop codons in *gvpA*) by monitoring the activity of both promoters simultaneously. These experiments confirmed the UAS of P_{pD}, but also the hypothesized GvpE–UAS of P_{pA} and proved that both UAS elements almost entirely overlap with their distal 8-nt portions in the centre of the P_{pD}–P_{pA} region. In addition, variations in the UAS–BRE distance, a complete substitution of the entire UAS element, and complete substitutions of either the distal or the proximal region were constructed. The results underlined that the close location of UAS–BRE is required for the GvpE-induced promoter activity.

MATERIALS AND METHODS

Constructs used for transformation of *H. volcanii* WFD11

The *H. volcanii* medium and growth conditions, the various E^{ex} constructs (*gvpE* fused to the ferredoxin promoter P_{fdx} in the expression vector pJAS35), and also the P_A–*bgaH* construct have been described (4,5,11). The construct *pA–pD* contains the leaderless p-*gvpA* reading frame fused to the P_{pA}–P_{pD} promoter region, and *bgaH* fused to the transcript start site of p-*gvpD* (without the p-*gvpD* mRNA leader region) in the *Escherichia coli* vector pBluescriptSK+. The *bgaH* reading frame includes six codons for additional amino acids at the N-terminus to ensure the production of an active BgaH enzyme (11). The construction of *pA–pD* involved the amplification of the leaderless p-*gvpA* in two PCR reactions using p-vac as template and the primer pairs 3′pD2ΔL–bgaH plus pA-Dlo-18, or 5′p-gvpA–XbaI plus pA-Dlu-18 (Table 1). The resulting subfragments served as templates in the third PCR with primer pair 5′p-gvpA-XbaI plus 3′pD2ΔL-bgaH to yield the fusion product that was used to substitute the P_{pA} promoter in P_{pA}–*bgaH*–pBluescriptSK+ resulting in $pA–pD_{\text{Bluescript}}$. This construct served (i) as template for the amplification of the XbaI–BamHI fragment P_{pD}–*bgaH* using the primers 3′-PpD(2) and 5′-PpD–HindIII (Table 1), (ii) for the construction of the initial $pApD_{\text{pWL102}}$ vector to investigate the activities of both oppositely oriented promoters that turned out to be not useful due to the GvpA production and (iii) as template to construct $pApD_{UGA}$ to investigate the P_{pA} and P_{pD} promotor activities simultaneously in *H. volcanii* transformants.

Table 1. Primers used to construct the P_{pD} and pApD promoter mutants

Primer	Sequence in 5′–3′ direction[a]
3′pD2ΔL-bgaH	CCAACTG*CCATGG*AATCTGGTTGCGC CATCTAAGAAGCTTTACACTCTCCG
pA-Dlo-18	TAGTTAGAGATGATGGCGCAACC
pA-Dlu-18	GGTTGCGCCATCATCTCTAACTA
5′-PpD-HindIII	GC*AAGCTT*GTGTATGGTTTCACCAGTC GTTATGTC
5′p-gvpA-XbaI	ATAGTAT*TCTAGA*CAAGCGATTCACCTCCC
3′-PpD(2)	CGTAAGGGAGGTGAATCGCTTG
3′-PpD (3)	GTGAAACCATACACAAGCTTGCCG
3′-PpD (4)	TACACAAGCTTGCCGTAAGGGAGGTG
5′-pD-M1	TGGTTTCACCAGTCGTTATGTCTCCTGTA **GATCA**TCGTACTTCTAAG
5′-pD-M2	TGGTTTCACCAGTCGTTATGTCTCC**CTCG** **G**TGAGTCGTACTTC
5′-PpD-M3II	TGGTTTCACCAGTCGTTATGT**ACAGC**GTA ATGAGTCGTAC
5′-pD-M4	TGGTTTCACCAGTCGTT**GGACA**TCCTGTA ATGAG
5′-pD-M5	TGGTTTCACCAGT**ATCCG**TGTCTCCT GTAATG
5′-PpD-M6	TGGTTTCAC**AGTGA**GTTATGTCTCCTG TAATG
5′-PpD-M7	TGGTT**GTCTA**AGTCGTTATGTCTCCTG TAATG
5′-PpD-M8	T**CTACG**CACCAGTCGTTATGTCTCCTG TAATG
5′-PpD-M9	GTGT**GGC**GTTTCACCAGTCGTTATG
3′-PpD-M9	ATCCTTATGTGATGCCCGAG
3′-PpA(WT)	TACACATCCTTATGTGATGCCC
gvpA + UGA 5′	CTTGTGAGTGATTGATGATCGTGTAC TAGAC
gvpA + UGA 3′	CGATCATCAATCACTCACAAGCCTGAA GAATCTG
5′-PpD + 3	CAGTCGTTATGTCTCCTGTAATGAGTG TTCGTACTTCTAAG
5′-PpD + 6	CAGTCGTTATGTCTCCTGTAATGAGGA CTGATCGTACTTCTAAG
5′-PpD-Δ3I	CAGTCGTTATGTCTGTAATGAGTCGTA CTTCTAAG
5′-PpD-Δ3II	CAGTCGTTATGTCTCCTGTAATTCGTAC TTCTAAG

[a]Substitutions marked in bold, insertions underlined, restriction sites in italics.

Table 2. Primers used to construct mutants with insertions, deletions or substitutions

Primer	Sequence in 5′–3′ direction[a]
mcA-XbaI	CCAAACTA*TCTAGA*TGTTTGAC
mcA-InsI-*forward*	CAACTGTACGAATGATTTTGTTAC
mcA-InsI-*reverse*	TCGTACAGTTGGTTCAGCAACC
mcA-InsII-*forward*	TTGCGACTGAACCAACACGAATG
mcA-InsII-*reverse*	TTCAGTCGCAACCGTTTCACCTC
mcA-Del-*reverse*	GTTCA/ACCGTTTCACCTCTCG
mcA-Del-*forward*	ACGGT/TGAACCAACACGAATGTGA
mcA-Sub-*forward*	GGGTCTCACCTTGCGTCTGATTGAC GAATGATTTTGTTAC
mcA-Sub-*reverse*	GTCAATCAGACGCAAGGTGAGACCCT
5′-Xba-PmcD	GCAAGTAACA*TCTAGA*TTCGTGTTGG TTCAGCAACCG
3′-Nco-pA(1-5)-PmcD	CTG*CCATGG*AATCTGGTTGCGCCATG GATGACGCAC
pA + 10nt 5′	CCATTGTGACTGAGACACATCCTTAT GTGATGCC
pA + 10nt 3′	GTGTCTCAGTCACAATGGTTTCACC AGTCGTTATG
5′-pA1 + 1	GG**CATAACGA**TACACATCCTTATGT GATGC
5′-pA2 + 2	GA**TGAAACCA**CTGGTGAAACCATAC ACATC
5′-pA1 + Δ2	GG**GTCTGATTG**ACACATCCTTATGT GATGC
5′-pAΔ1 + 2	GA**GTCTCACC**CTGGTGAAACCATAC ACATC
3′-pA1	AGTCGTTATGTCTCCTGTAATGAGTC
3′-pA2	TCCTGTAATGAGTCGTACTTCTAAG TACG

[a]Substitutions marked in bold, insertions underlined, slash marks position of deletion, restriction sites in italics.

The P_{pD}–*bgaH* fragment inserted into pWL102 served as wild type in the P_{pD} mutation studies. The P_{pD}–*bgaH* promoter mutants *pD-M1* through *pD-M8* each contained a 5-nt substitution upstream of P_{pD}–BRE. All mutants were constructed by PCR using P_{pD}–*bgaH* in pBluescriptSK + as template and primer 3′-PpD(4) plus the respective 5′-mutation primer harbouring the 5-nt substitutions (Table 1). The promoter mutants *pD + 3*, *pD + 5*, *pDΔ3I* and *pDΔ3II* with insertions or deletions upstream of BRE were constructed using P_{pD}–*bgaH* and primer 3′-PpD(3) plus the respective 5′ mutation primers (Table 1). All mutant-P_{pD}–*bgaH* fragments were transferred to pWL102 as XbaI–BamHI fragment.

Construct $pApD_{UGA}$ (3 UGA-stop codons introduced in p-*gvpA* starting at position 28) was constructed using primer pair gvpA-UGA-5′ and gvpA-UGA-3′ for the PCR (Table 1). Promoter mutants harbouring 5-nt substitutions (*pApD–M1* through *M8*, identical to those described for pD above) and an additional mutant *pApD–M9* were constructed by PCR using $pApD_{UGA}$ as template together with primer 3′-PpA(WT) or 3′PpD–M9 plus the respective 5′-mutation primer 5′-PpD–M1 through M9 (Table 1). The resulting XbaI–BamHI *gvpA–*P_{pA}*-*P_{pD}*–bgaH* fragments were transferred to pWL102 and used to transform *H. volcanii*.

The P_{pA}–*bgaH* mutant *pA1 + 1* (substitution of the proximal UAS portion 2 by portion 1) and *pA1 + Δ2* (proximal UAS portion mutated) were produced by PCR using pA–*bgaH* in pBluescriptSK + as template and primer 3′-pA1 plus the mutation primers 5′-pA1 + 1 or 5′-pA1 + Δ2 (Table 2). Similarly, the mutants *pA2 + 2* (substitution of UAS portion 1 by 2) and *pAΔ1 + 2* (mutation of the UAS portion 1) were constructed using P_A–*bgaH* as template and primer 5′-pA2 plus the mutation primers 5′-pA2 + 2 or 5′-pAΔ1 + 2 (Table 2). Construct *pA + 10* contains a 10-nt insertion between UAS and BRE and was constructed using P_A–*bgaH* as template and primer pair pA + 10nt-5′ and pA + 10nt-3′ (Table 2).

The P_{mcA}–*bgaH* mutants were constructed in a similar way by PCR. Mutant *mcA–InsI* (TGT-insertion adjacent to BRE) was constructed using primer pair mcA–XbaI and InsIforward for the first PCR, and mcA–NcoI2a and InsI-reverse for the second PCR (Table 2). The third PCR was done with primers mcA–XbaI and mcA–NcoI2a. The *mcA–InsII* mutant was produced using primers InsII-forward and InsII-reverse together with the primers mcA–XbaI and mcA–NcoI2a (Table 2). Construct *mcA–Del* was

produced using the primers Del-reverse and Del-forward, and construct *mcA–Sub* using Sub-reverse and Sub-forward. Construct $P_{mcD}L$–*bgaH* was obtained using the mc-vac region in pBluescriptSK + as template and primer pair 5′-Xba–PmcD and 3′-Nco–pA(1–5)-PmcD (Table 2). The fragment contains the P_{mcD} promoter region plus the region encoding the mRNA leader of mc-*gvpD*. All these promoter fragments were fused as XbaI–NcoI fragments to the *bgaH* reading frame in pBluescript and transferred as XbaI–BamHI fragment to pWL102 that was used to transform *H. volcanii*. All promoter sequences and fusions were controlled by DNA sequencing. The accession numbers of the p-vac subfragmentsin Genbank are X64729 (p-*gvpACNO*), X55648 (p-*gvpDEFGHIJKLM*) and X64701 of the mc-vac region.

Selection of transformants and BgaH assays

Prior to the transformation of *H. volcanii* each construct was passaged through the *E. coli dam*$^-$ strain GM 1674 to avoid a halobacterial restriction barrier. Transformation was done as described (15), and transformants were selected on agar plates containing 6 μg mevinolin ml^{-1} (pWL102) and/or 0.2 μg novobiocin ml^{-1} (pJAS35). Mevinolin is a derivative of lovastatin that was obtained as a generous gift of MSD Sharp & Dohme GmbH (Haar, Germany). The amount and presence of the desired constructs in each transformant were controlled by the analysis of the isolated plasmids. The BgaH activity was measured by ONPG assay in cell lysates of the respective *bgaH* transformants (16). The protein concentration was determined by the Bradford assay (17) using BSA as standard.

Isolation of RNA and transcript analysis

RNA was isolated from *H. volcanii* transformants according to (18) from cultures at OD_{600} = 1.8–2.0. Northern analyses involved electrophoresis of 2 or 0.02 μg RNA on denaturing, formaldehyde-containing, 1.2% (w/v) agarose gels, followed by capillar transfer to nylon membranes (17). A strand-specific RNA probe complementary to *bgaH* mRNA was synthesized using the 2.2-kb *bgaH* fragment inserted in pBluescriptSK + as template for T7 polymerase. Similarly, a strand-specific p-*gvpA* RNA probe was produced using p-*gvpA* inserted in pBluescriptSK + . The RNA was labelled using the DIG RNA Labeling Kit (Roche, Germany). Northern hybridization was carried out as described by Ausubel *et al*. (17), but the hybridization solution contained 10% (w/v) dextran sulphate (Sigma, Germany), 1% (w/v) SDS and 0.5% (w/v) skim milk powder.

Western analysis and DNA sequence analysis

Samples of *H. volcanii* and *H. volcanii* transformants were taken in early stationary growth (after 48–54 h of growth) and processed for protein isolation as described (6). Soluble proteins (20 μg) were separated on 12% tricine SDS–polyacrylamide gels (19). Western analyses were performed as described (17). Two different antisera raised against cGvpE (10) and mcGvpE (4) were used in a dilution of 1:1000 (mcGvpE) or 1:10000 (cGvpE antiserum) in blocking buffer, and the reacting antibodies were detected using the ECL detection system (GE Healthcare, Germany). DNA sequence determination of the fusion constructs was done according to the Sanger method using the Sequi-Therm EXCEL II Long-Read DNA Sequencing Kit-LC protocol (Biozym, Germany). The fragments were separated using a Licor DNA sequencer.

RESULTS

Stimulation of the P_{pD} promoter activity by three different GvpE proteins

In silico analysis of the region upstream of P_{pD} (and P_{mcD}) indicated a sequence element related to the UAS of P_{mcA} that could be a putative GvpE-responsive element (Figure 1C). In contrast, the P_{cD} promoter of c-vac lacking the activation by GvpE did not show such a conserved sequence element (Figure 1C). An initial $P_{mcD}L$–*bgaH* construct (containing P_{mcD} plus the region encoding the mRNA leader of mc-*gvpD* fused to *bgaH*) did not yield detectable BgaH activities in *H. volcanii* transformants. However, the P_{pD}–*bgaH* construct containing the direct fusion of the *bgaH* reading frame to P_{pD} ('leaderless') was useful. Transformants containing P_{pD}–*bgaH* together with pE^{ex} (p-*gvpE* reading frame expressed under ferredoxin promoter control) produced well detectable amounts of BgaH (35 mU/mg protein). To determine the P_{pD} activity in response to the two other GvpE proteins, cGvpE and mcGvpE, P_{pD}–*bgaH* was tested in transformants carrying cE^{ex} or mcE^{ex}. The presence of each GvpE protein was confirmed by western analyses using an antiserum raised against cGvpE (10). The basal P_{pD} promoter activity measured as BgaH activity in the lysate of the P_{pD}–*bgaH* transformants was with 1.2 mU/mg rather low, but much larger GvpE-induced activities were observed in the lysates of transformants harbouring in addition to P_{pD}–*bgaH* construct pE^{ex} (35 mU/mg), mcE^{ex} (410 mU/mg) or cE^{ex} (830 mU/mg). These results suggested that cGvpE was the strongest and pGvpE the weakest activator protein, similar to the results already described for the P_{mcA} and P_{pA} promoters (9,11).

Substitution mutagenesis to identify the UAS of the P_{pD} promoter

A 5-nt scanning mutagenesis was performed with P_{pD}–*bgaH* to identify the UAS element required for the GvpE-mediated activation of P_{pD}. The mutations started upstream of the P_{pD}–BRE and extended to the BRE of the oppositely oriented P_{pA} promoter (Figure 2C). The P_{pA}–TATA-box and further p-*gvpA* gene sequences were not present in this construct to exclude any activity derived from P_{pA}. Eight mutants (*pD-M1* through *pD-M8*) were obtained and investigated for their BgaH activities in *H. volcanii* transformants (Figure 2A and C). Transformants harbouring the wild-type (or mutant) P_{pD}–*bgaH* construct plus the native pJAS35 (i.e. without *gvpE)* were used to determine the respective basal P_{pD} promoter activities, and P_{pD}-*bgaH* + pE^{ex} transformants were used to quantify the pGvpE-induced promoter activities. In each case, the presence of pGvpE was

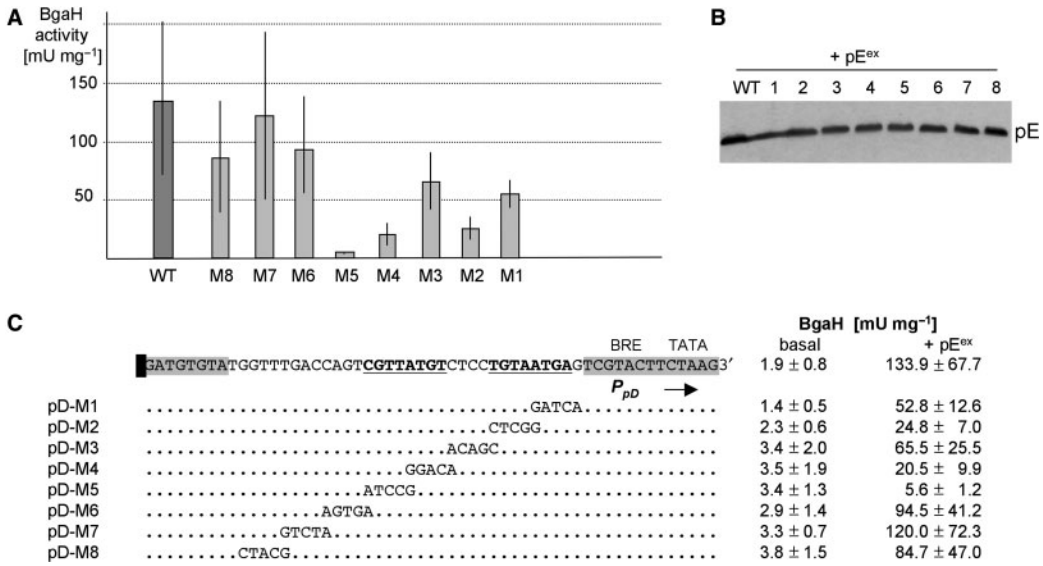

Figure 2. Analysis of mutants derived from P_{pD}–*bgaH*. (**A**) BgaH activities determined for the P_{pD}–*bgaH* wild type and the mutants in P_{pD}–*bgaH* + pE^{ex} transformants, including standard deviations ($n = 4$). (**B**) Western analysis to confirm the presence of similar amounts of pGvpE in each of these transformants. The label pE depicts GvpE. (**C**) Sequence of the intergenic region of p-vac with the two oppositely located BRE elements and P_{pD}–TATA-box shaded in grey. The arrow points in the direction of P_{pD} transcription. The UAS element determined for P_{pD} is underlined. Dots in the lines underneath depict nucleotides identical to wild type, and the respective nucleotide substitutions are given. The basal and GvpE-induced activities quantified by BgaH assay are given on the right.

assessed by western analysis using the antiserum raised against cGvpE, and all of them contained pGvpE in comparable amounts (Figure 2B). Similar basal promoter activities (<3.8 mU/mg protein) were determined for the wild-type P_{pD} and all P_{pD} mutants, indicating that none of these mutations affected the basal promoter activity. With respect to the GvpE-mediated activation, similar BgaH activities as found for wild-type (>84 mU/mg protein) were observed with the *pD-M6*, *M7* and *M8*, all of which harboured the mutation upstream of the putative P_{pD}–UAS element and close to the opposite P_{pA}–BRE (Figure 2A and C). Mutants with the alteration closer to P_{pD}–BRE yielded reduced BgaH activities. The strongest reductions were found for *pD-M5*, *M4* and *M2*, whereas only a minor reduction was observed for *pD-M3* carrying the alterations in the 4-nt non-conserved sequence between the two hypothesized 8-nt UAS portions (Figure 2A and C). A minor reduction was also observed with *pD-M1* (nucleotide substitutions adjacent to P_{pD}–BRE). These results proved the existence of the expected 20-nt P_{pD}–UAS consisting of two 8-nt portions. Alterations in the distal 8-nt portion of the P_{pD}–UAS (*pD-M5*, *M4*) imposed a stronger effect on the P_{pD} promoter activity than alterations in the proximal 8-nt portion (*pD-M2*, M1) (Figure 2A). In summary, the region affecting the GvpE-mediated activation of P_{pD} corresponded very well to the putative UAS element deduced from the comparison to P_{mcA}.

Substitution mutagenesis and simultaneous activation of P_{pD} and P_{pA}

A similar 5-nt scanning mutagenesis was performed using a dual reporter gene construct containing the native P_{pA}–P_{pD} promoter region. The initial *pApD* construct harboured this promoter region with P_{pD} fused to *bgaH* and P_{pA} to the leaderless p-*gvpA* reading frame. Transformants containing *pApD* by itself were obtained in large numbers, but only a few colonies of the *pApD* + pE^{ex} transformants were found. All of them produced a low level of BgaH (7 mU/mg; pApD, Figure 3A) and contained strongly reduced amounts of the plasmids (data not shown). Most likely these transformants were unable to tolerate the large amounts of the hydrophobic GvpA protein produced after the induction by pGvpE. To circumvent this problem, three UGA stop codons were introduced in all three reading frames in the 5′ region of p-*gvpA* in *pApD* to prevent the translation of the p-*gvpA* mRNA. The transfomants containing $pApD_{UGA}$ + pE^{ex} were easily obtained and produced the expected enhanced amounts of BgaH (UGA, Figure 3A). This $pApD_{UGA}$ construct was used as template for the 5-nt scanning mutagenesis encompassing the 35-nt of intervening sequences located between P_{pA}–BRE and P_{pD}–BRE. The nucleotides altered in constructs *pApD-M1* through *pApD-M8* were identical to the ones altered in the *pD-M1* through *pD-M8*, and for completion mutant *pApD-M9* with an alteration close to P_{pA}–BRE was constructed (Figure 3B). All these $pApD_{UGA}$ mutant constructs were investigated in *H. volcanii* transformants in the presence or absence of pE^{ex}. The P_{pD} promoter activities were determined by ONPG assays, and northern analysis was performed to determine the amounts of the p-*gvpA* transcript indicative for the P_{pA} activity. The presence of pGvpE was assessed by western analysis using the antiserum raised against cGvpE, and all of the pE^{ex} transformants contained pGvpE in comparable amounts (data not shown).

The basal P_{pD} promoter activities of the $pApD_{UGA}$ wild-type and mutant constructs were 5–20 mU/mg (data

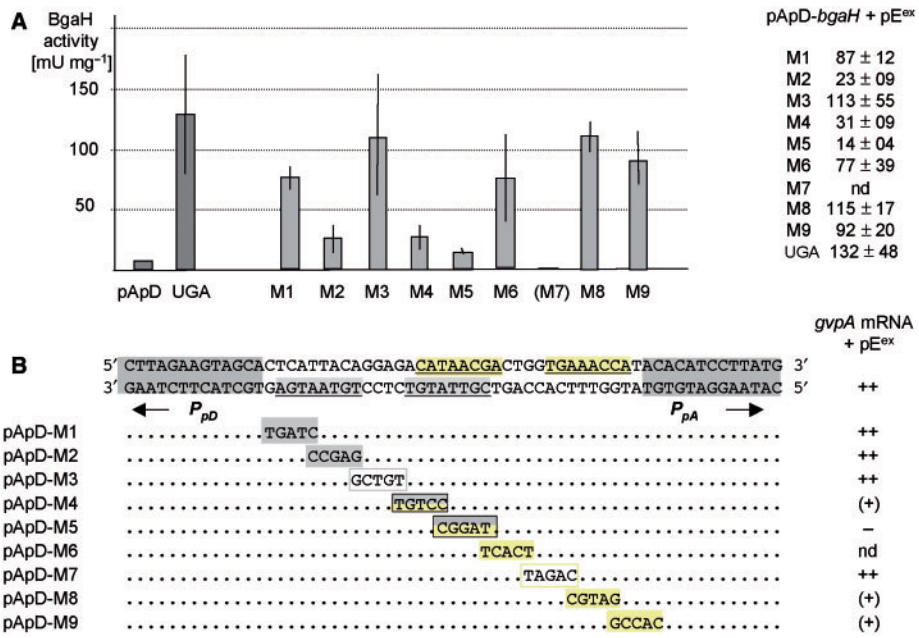

Figure 3. Analysis of *pApD* and of mutants derived from the dual reporter construct $pApD_{UGA}$. (**A**) BgaH activities determined for the P_{pD}–*bgaH* in $pApD_{UGA}$ + pE^{ex} wild type and mutants, including the standard deviations ($n = 4$). *pApD* designates the original construct, and UGA the construct containing the 3 UGA stop codons in p-*gvpA*. The GvpE-induced activities quantified by BgaH assay are given on the right. (**B**) Sequence of the P_{pD}–P_{pA} promoter region (given in opposite orientation as in Figure 2) with the two BRE elements and TATA-boxes shaded in grey. The arrows point to the directions of transcription. The two UAS elements determined are underlined, and the UAS of P_{pA} is shaded in yellow. The various nucleotide substitutions are indicated underneath, and dots depict identical sequences. The mutations were identical to the ones introduced into the promoter region of P_{pD}–*bgaH* (Figure 2). The mutations affecting P_{pD} are shaded in grey, and mutations affecting P_{pA} are shaded in yellow. The relative amounts of p-*gvpA* mRNA in the transformants + pE^{ex} (as determined by northern analysis, Figure 4) are given on the right. (+) = presence and (–) = absence of *gvpA* mRNA.

not shown). Only mutant *pApD-M7* did not yield any basal P_{pD} promoter activity, although the *bgaH* mRNA was observed in a comparable amount (data not shown). Since the *pApD-M7* + pE^{ex} transformant did not show any BgaH activity as well, we assumed that construct *pApD-M7* was defect in the production of an active BgaH (Figure 3A). The other eight $pApD_{UGA}$-mutant constructs confirmed the results described above for the various P_{pD}–*bgaH* mutants: *pApD-M3* (intervening 4-nt sequence altered) and *pApD-M6*, *M8* and *M9* (mutations upstream of the P_{pD}–UAS) yielded similar GvpE-induced P_{pD} activities as found for the wild-type $pApD_{UGA}$ (Figure 3A). Again, the strongest reductions in the BgaH activities were observed with mutants *pApD-M5*, *M4* and *M2* (<31 mU/mg). All these results confirmed the 20-nt UAS upstream of the P_{pD}–BRE as important for the GvpE-induced P_{pD} activity.

Total RNA was isolated from each transformant and northern analysis carried out to assess the activity of P_{pA} (Figure 4). The stable 320-nt p-*gvpA* transcript is always produced in large amounts. Thus, only 0.02 µg of total RNA were applied in each case for better visualization of the differences. The analysis of the basal transcription (without GvpE-stimulation) yielded similar amounts of p-*gvpA* mRNA except for the *pApD-M6* transformants that did not produce p-*gvpA* mRNA (data not shown). This mutant also lacked the GvpE-induction and was thus regarded as being defective (Figure 4). With respect to the GvpE-mediated induction of P_{pA} in the other mutants, the transformants *pApD-M1, M2* and *M3* contained

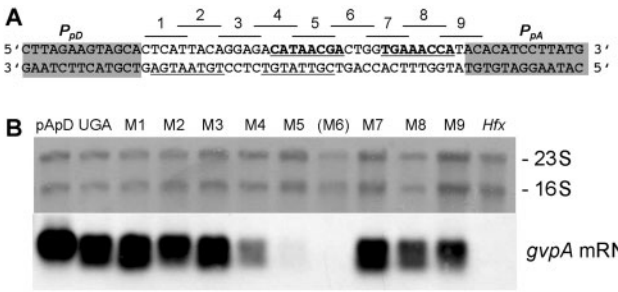

Figure 4. Northern analysis to determine the amount of p-*gvpA* mRNA in $pApD_{UGA}$ + pE^{ex} transformants. (**A**) Nucleotide sequence of the P_{pD}–P_{pA} promoter region with the two BRE elements and TATA-boxes shaded in grey. The two UAS elements are underlined. Lines and numbers above the sequence depict the various 5-nt mutations in mutants *pApD-M1* through *M9*. (**B**) Total RNA of 0.02 µg (bottom) derived from each transformant were separated on a formaldehyde containing, 1.2% agarose gels and hybridized a *gvpA*-specific probe. Amounts and quality of the RNA were checked by staining the 16S and 23S RNA (top; 2 µg RNA applied in this case).

similar amounts of p-*gvpA* mRNA as found for wild-type $pApD_{UGA}$ indicating that the region altered in these mutants was not important for the GvpE-mediated activation of P_{pA}. These mutations were located upstream of the putative 20-nt P_{pA}–UAS and close to P_{pD}–BRE (Figures 3B and 4A). The strongest reduction in the amount of p-*gvpA* mRNA was seen with mutants *pApD-M5* and *M4*, whereas less strongly reduced amounts of

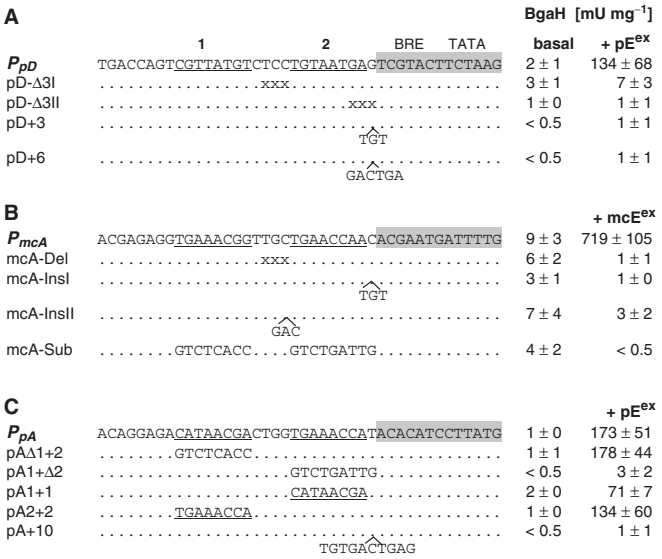

Figure 5. Distance variants constructed for the P_{pD} (**A**), P_{mcA} (**B**) or P_{pA} (**C**) promoter region. The sequence of each promoter region is given on top, with TATA-box and BRE shaded in grey. The UAS elements are underlined. Dots in the lines underneath depict nucleotides identical to wild type. Deletions are marked by xxx, and substitutions or insertions are indicated. The basal and GvpE-induced promoter activities quantified by BgaH assay are given on the right.

p-*gvpA* mRNA were detectable in mutants *pApD-M8* and *M9*. Mutant *pApD-M7* produced almost similar amounts as the wild-type $pApD_{UGA}$ (Figure 4B). These results confirmed the P_{pA}–UAS derived from the comparison with P_{mcA} (Figure 1C), and also demonstrated the simultaneous use of both 20-nt UAS elements in $pApD_{UGA}$ (Figure 3B). The overlapping distal portions of both elements in the centre of this region were most sensitive with respect to mutations affecting the GvpE-mediated activation. The region altered in mutant *M5* led to the lack of both P_{pD} and P_{pA} promoter activities and proved to be very important for the expression of both *gvp* genes.

Distance variants of the UAS and effect of a complete substitution

To determine whether the size of the 4-nt region between the two 8-nt portions, and also the close location of UAS and BRE were important for the GvpE-mediated activation, distance variants were constructed using P_{pD}-, P_{mcA}- and P_{pA}–*bgaH* constructs (Figure 5). The UAS of P_{pD}–*bgaH* was altered by two different 3-nt deletions, one introduced in the 4-nt intervening sequence (mutant *pDΔ3I*) and the other one adjacent to BRE (*pDΔ3II*). Two additional mutants carried a 3- or 6-nt insertion next to BRE (*pD+3, pD+6*). Mutant *pDΔ3I* (deletion in the intervening sequence) showed a normal basal P_{pD} promoter activity, but almost no induction by GvpE, suggesting that the size of the space between the two 8-nt portions of the UAS cannot be altered without loosing the GvpE-mediated activation (Figure 5A). The mutants *pDΔ3II*, *pD+3* and *pD+6* with alterations adjacent to BRE yielded very low basal P_{pD} activities in transformants, implying that the nucleotides adjacent to BRE are still important for the initiation of basal transcription. None of these promoters was inducible by GvpE, demonstrating that the distance between UAS and BRE cannot be altered (Figure 5A). Even a 10-nt (= 1 helix turn) insertion between the UAS and BRE performed with P_{pA}–*bgaH* resulted in the lack of the GvpE-mediated activation (Figure 5C).

Similar analyses were performed with the P_{mcA}–*bgaH* construct containing the P_{mcA} promoter of *H. mediterranei* (Figure 5B). Two 3-nt insertions enlarged the distance between UAS and BRE (*mcA–InsI*), or the space between the two 8-nt portions (*mcA–InsII*). Both mutants showed a normal basal promoter activity in P_{mcA}–*bgaH* transformants, but all of them lacked the induction mediated by mcGvpE (Figure 5B). A 3-nt deletion in the spacer between the two 8-nt UAS portions (*mcA–Del*) led to the loss of the GvpE-induced activity (Figure 5B), similar to the results obtained with P_{pD} (Figure 5A). Altogether, these results demonstrated that the 4-nt distance between UAS-portions 1 and 2 and a close location of the 20-nt UAS to BRE are crucial for the GvpE-mediated activation. Mutant *mcA-Sub* contained a completely substituted P_{mcA}–UAS element (Figure 5B). No effect was observed on the basal P_{mcA} activity, but the GvpE-mediated activation was completely abolished, demonstrating that the UAS-element is indeed essential for the GvpE-mediated activation.

Alteration of the proximal or distal 8-nt portion of the UAS

Four additional mutants were constructed with P_{pA}–*bgaH* to determine the effect of alterations in the two 8-nt portions 1 or 2 on the GvpE-induced expression (Figure 5C). Mutants *pA1+Δ2* and *pAΔ1+2* contained one of the 8-nt portions completely substituted, and *pA1+1* and *pA2+2* contained two identical 8-nt portions of the UAS (Figure 5C). The basal P_{pA} promoter activities (determined in the presence of the 'empty' vector pJAS35 in the respective transformants) were in the range of the P_{pA}–*bgaH* transformant or at the detection limit (0.5 mU/mg), indicating that the basal transcription was not affected (Figure 5C). With respect to the GvpE-induction, *pAΔ1+2* transformants yielded a BgaH activity similar to wild type, suggesting that the proximal 8-nt portion located close to BRE was sufficient for the activation in this single promoter construct. In contrast, the P_{pA} promoter in *pA1+Δ2* was not activated by GvpE underlining that UAS and BRE must be in close contact. The two constructs containing the identical 8-nt portions of the UAS (*pA1+1* and *pA2+2*) yielded slightly reduced (*pA2+2*, 72% of the BgaH activity of wild type) or stronger reduced GvpE-induced activities (*pA1+1*, 40%) (Figure 5C). The latter result could be due to the fact that the UAS portion 1 is active in both orientations, and a location of this element next to BRE might disturb the direction of the GvpE-mediated activation of P_{pA}. These results underlined that both UAS portions were not equal in function, and that one of these UAS portions was required in close contact to BRE to yield a GvpE-stimulated promoter activity.

DISCUSSION

In this report, we investigated the sequences required for the GvpE-mediated activation of the two oppositely oriented promoters, P_A and P_D, driving the expression of the two *gvp* gene clusters involved in the gas vesicle formation. A scanning mutagenesis previously performed with the related P_{mcA} of the mc-vac region determined a 20-nt sequence adjacent to P_{mcA}–BRE sequence as important for the GvpE-mediated activation (13). This 20-nt sequence appears to be conserved between the three different P_A promoters (Figure 1). A putative P_{pD}-UAS should be located at a similar position upstream and adjacent to BRE, and *in silico* analysis yielded related, but slightly divergent sequences for the two GvpE-activated P_D promoters in mc-vac and p-vac.

The UAS element required for the GvpE-induction of P_{pD} was determined by scanning mutagenesis with P_{pD}–*bgaH* using eight different 5-nt mutations, and all these variants were investigated in *H. volcanii* transformants in the presence (+pE^{ex}) or absence of pGvpE. None of these mutations abolished the basal transcription initiated at P_{pD}, and the analysis of the transformants containing pE^{ex} in addition clearly defined the region required for the GvpE-mediated activation. As expected, this region was found close to the P_{pD}–BRE and consisted of two 8-nt sequence portions spaced by four non-conserved nucleotides. Any mutations further upstream did not affect the GvpE-induction of P_{pD}. Additional mutants constructed to determine the effect of distance variations showed that the spaces between UAS–BRE and also between the two 8-nt UAS portions were important. Similar results were also observed with distance variants of the P_{mcA}–UAS, where a 3-nt deletion, or several insertions between UAS and BRE resulted in the loss of the GvpE-mediated promoter activation. Thus, a very close location of UAS and BRE is required for the GvpE-mediated activation. In addition, mutants harbouring a complete substitution of the P_{mcA}–UAS lacked the activation by GvpE, indicating that the UAS sequence was essential for the GvpE-induced promoter activation. The consensus sequence YGAAAYGA could be derived from all 8-nt portions of the UAS elements found in the various *gvp* promoters activated by GvpE. This sequence is specific for the *gvp* gene clusters and does not occur throughout the genome sequence of *H. salinarum* NRC-1 (20). The close location of UAS and BRE suggests that GvpE could contact proteins of the basal transcription apparatus. It is possible that GvpE enhances the recruitment of TBP and thus activates the transcription initiation, similar to the transcriptional activator Ptr2 of *Methanocaldococcus jannaschii* (21,22).

Due to the 35-nt intervening sequence between the BRE sequences of P_D and P_A, the distal portions of both 20-nt UAS elements almost completely overlap in the centre of the region. The dual reporter construct $pApD_{UGA}$ was used to analyse the activity of both promoters simultaneously. The P_{pD}–UAS element determined by the scanning mutagenesis in $pApD_{UGA}$ was identical to the one determined for P_{pD}–*bgaH*, and the northern analysis done with a p-*gvpA*-specific probe

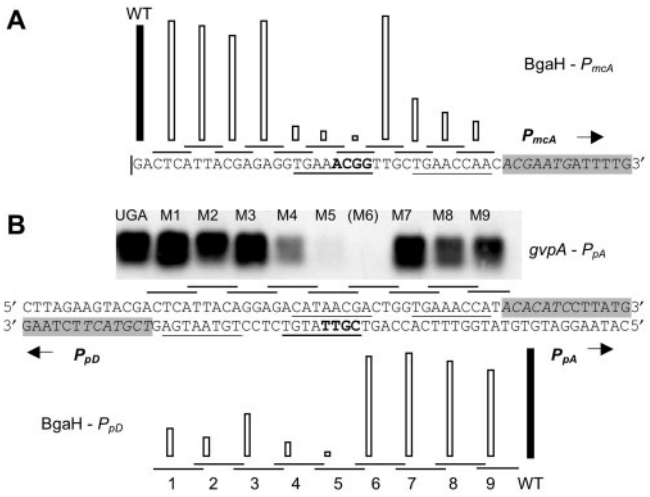

Figure 6. Comparison of the various scanning mutageneses performed with the mc-vac (**A**) and p-vac (**B**) promoter regions. The columns above the sequences indicate the specific BgaH activities determined for the various mutants (13, and this study). The respective mutations are marked as lines below each column and include the numbers of the various $pApD_{UGA}$ mutants in (B). The 8-nt portions of each 20-nt UAS element are underlined, and the TATA-box and BRE are shaded in grey. Arrows point in the direction of transcription. The 4-nt next to the centre of the region that were the most important ones for the GvpE-mediated activation of both promoters are indicated in bold.

confirmed the P_{pA}–UAS element for P_{pA} that was predicted from the comparison with the P_{mcA} promoter region. These analyses also uncovered interesting features concerning the use and also the importance of the two 8-nt UAS portions. The mutations in both portions affected the GvpE-induced activation of the two promoters in slightly different ways. The activation of P_{pA} by GvpE was more severely affected when the mutation occurred in the 3′-region of the central 8-nt portion, whereas in the case of P_{pD} the alterations in the 5′-region of this UAS portion were more effective (Figure 6). The strongest effect on the GvpE-enhanced promoter activity was observed with mutants carrying 4- or 5-nt alterations in this distal 8-nt portion of the UAS element, that thus appeared to be the most important one in the dual promoter construct (Figure 6). A 4-nt sequence could be assigned in the central region where alterations most strongly affected the P_{pD}-, P_{pA}- or P_{mcA} activities; this region is located next to centre and closer to P_A (Figure 6A and B, marked in bold). The sequence constitutes the 3′- (P_A) or the 5′-portion (P_D) of the respective overlapping distal 8-nt UAS portions. This region might be required for the initial binding of GvpE, followed by the occupancy of the respective proximal 8-nt portions of the UAS. In contrast, alterations in the proximal 8-nt portion were less severe on the GvpE-induced promoter activity (Figure 6B). The results obtained with the dual promoter construct were very similar to the results obtained with the two single promoter constructs P_{mcA}–*bgaH* (11) and P_{pD}–*bgaH* (this study), and demonstrated that both UAS elements including the overlapping portions are indeed functional in $pApD_{UGA}$. Despite the fact that mutation of UAS portion 1 imposed the strongest effect on the

promoter activation by GvpE, this distal portion of the UAS could be deleted without the loss of the GvpE-mediated activation in the single promoter construct *pAΔ1+2*. The reason for this discrepancy is still unclear. In contrast, construct *pA1+Δ2* (lacking the proximal UAS portion) did not respond to GvpE, underlining the importance of a close location of at least one UAS portion and BRE for the activation by GvpE.

The promoter mutants carrying an UAS consisting of two identical portions yielded a slight reduction of the GvpE-induced activity (72%) in the case of *pA2+2*, whereas the *pA-1+1* promoter version resulted in only 40% of the GvpE-induced activity determined for wild type. The latter result implied that the possible use of UAS-portion 1 in two orientations somehow disturbs the recruitment of the basal transcription apparatus by GvpE, if this sequence is placed adjacent to BRE.

In summary, our results confirmed the almost complete overlap of the two distal portions of both UAS regulatory elements in the P_D–P_A promoter region. This arrangement appears to be similar to overlapping operator sequences in the genome of bacteriophage lambda. To our knowledge, this is the first case of such an arrangement of regulatory elements in Archaea. Another promoter region, containing two oppositely oriented promoters that are co-ordinately regulated, has been characterized for the genes encoding the selenium-free [NiFe]-hydrogenases in *Methanococcus voltae*, but the distance between both TATA-boxes is with 290-nt significantly larger (23). The compact arrangement of the regulatory elements in P_A–P_D might determine the amount and the time point for the activation of the both divergent *gvp* promoters during the gas vesicle formation, and it might be interesting to investigate the activity of both P_A and P_D promoters with the natural UAS-overlap compared to a construct harbouring two separated UAS elements with respect to the time-resolved expression during growth.

ACKNOWLEDGEMENTS

We thank Sandra Scheuch, Katharina Teufel, Torsten Hechler for valuable discussions and critical reading of the manuscript. Lovastatin was a generous gift of MDS Sharp & Dohme (Haar, Germany). This work was financially supported by the German Research Foundation, DFG (Pf 165/9-2). Funding to pay the Open Access publication charges for this article was provided by TU Darmstadt.

Conflict of interest statement. None declared.

REFERENCES

1. Röder,R. and Pfeifer,F. (1996) Influence of salt on the transcription of the gas vesicle genes of *Haloferax mediterranei* and identification of the endogenous transcriptional activator gene. *Microbiology*, **142**, 1715–1723.
2. Englert,C., Krüger,K., Offner,S. and Pfeifer,F. (1992) Three different but related gene clusters encoding gas vesicles in halophilic archaea. *J. Mol. Biol.*, **227**, 586–592.
3. Plößer,P. and Pfeifer,F. (2002) A bZIP protein from halophilic archaea: structural features and dimer formation of cGvpE from *Halobacterium salinarum*. *Mol. Microbiol.*, **45**, 511–520.
4. Zimmermann,P. and Pfeifer,F. (2003) Regulation of gas vesicle formation in *Haloferax mediterranei*: the two regulatory proteins GvpD and GvpE interact. *Mol. Microbiol.*, **49**, 783–794.
5. Pfeifer,F., Zotzel,J., Kurenbach,B., Röder,R. and Zimmermann,P. (2001) A p-loop motif and two basic regions in the regulatory protein GvpD are important for the repression of gas vesicle formation in the archaeon *Haloferax mediterranei*. *Microbiology*, **147**, 63–73.
6. Scheuch,S. and Pfeifer,F. (2007) GvpD-induced breakdown of the transcriptional activator GvpE of halophilic archaea requires a fundcitonal p-loop and an arginine-rich region of GvpD. *Microbiology*, **153**, 947–958.
7. Littlefield,O., Korkhin,Y. and Sigler,P. (1999) The strucutral basis for the oriented assembly of a TBP/TFB/promoter complex. *Proc. Natl Acad. Sci. USA*, **96**, 13668–13673.
8. Bell,S.D., Kosa,P., Sigler,P. and Jackson,S. (1999) Orientation of the transcription preinitiation complex in Archaea. *Proc. Natl Acad. Sci USA*, **96**, 13662–13667.
9. Hofacker,A., Schmitz,K., Cichonczyk,A., Sartorius-Neef,S. and Pfeifer,F. (2004) GvpE- and GvpD-mediated transcription regulation of the p-*gvp* genes encoding gas vesicles in *Halobacterium salinarum*. *Microbiology*, **150**, 1829–1838.
10. Krüger,K. and Pfeifer,F. (1996) Transcript analysis of the c-vac region, and differential synthesis of the two regulatory gas-vesicle proteins GvpD and GvpE in *Halobacterium salinarium* PHH4. *J. Bacteriol.*, **178**, 4012–4019.
11. Gregor,D. and Pfeifer,F. (2001) The use of a halobacterial *bgaH* reporter gene to analyse the regulation of gene expression in halophilic archaea. *Microbiology*, **147**, 1745–1754.
12. Holmes,M. and Dyall-Smith,M. (2000) Sequence and expression of a halobacterial β-galactosidase gene. *Mol. Microbiol.*, **36**, 114–122.
13. Gregor,D. and Pfeifer,F. (2005) *In vivo* analyses of constitutive and regulated promoters in halophilic archaea. *Microbiology*, **151**, 25–33.
14. Kosa,P., Ghosh,G., DeDecker,B. and Sigler,P. (1997) The 2.1 Å crystal structure of an archaeal preinitiation complex: TATA box-binding protein/transcription factor (II)B core/TATA box. *Proc. Natl Acad. Sci. USA*, **94**, 6042–6047.
15. Pfeifer,F. and Ghahraman,P. (1993) Plasmid pHH1 of *Halobacterium salinarum*: characterization of the replicon region, the gas vesicle gene cluster and insertion elements. *Mol. Gen. Genet.*, **238**, 193–200.
16. Holmes,M., Scopes,, R. Moritz.,R., Simpson,R., Englert,S., Pfeifer,F. and Dyall-Smith,M. (1997) Purification and analysis of an extremely halophilic beta-galactosidase from *Haloferax alicantei*. *Biochim. Biophys. Acta*, **1337**, 276–286.
17. Ausubel,F., Brent,R., Kingston,R., Moore,D., Seidman,J., Smith,J. and Struhl,K. (1988) *Current Protocols in Molecular Biology*, Vol. 1. Greene Publishing Associates and Wiley-Interscience, NY.
18. Chomczynski,P. and Sacchi,N. (1987) Single step method of RNA isolation by acid guanidinium thiocyanate-phenol-chloroform extraction. *Anal. Biochem.*, **162**, 156–159.
19. Schägger,H. and von Jagow,G. (1987) Tricine-sodium dodecyl sulfate-polyacrylamide gel electrophoresis for the separation of proteins in the range from 1 to 100 kDa. *Anal. Biochem.*, **166**, 368–379.
20. Ng,W., Kennedy,S., Mahairas,G., Berquist,B., Pan,M., Shukla,H., Lasky,S., Baliga,N., Thorsson,V. *et al.* (2000) Genome sequence of *Halobacterium* species NRC-1. *Proc. Natl Acad. Sci. USA*, **97**, 12176–12181.
21. Ouhammouch,M., Dewhurst,R., Hausner,W., Thomm,M. and Geiduschek,E. (2003) Activation of archaeal transcription by recruitment of the TATA-binding protein. *Proc. Natl Acad. Sci. USA*, **100**, 5097–5102.
22. Ouhammouch,M., Langham,G., Hausner,W., Simpson,A., El-Sayed,N. and Geiduschek,E. (2005) Promoter architecture and response to a positive regulator of archaeal transcription. *Mol. Microbiol.*, **56**, 625–637.
23. Noll,I., Müller,S. and Klein,A. (1999) Transcriptional regulation of genes encoding the selenium-free [NiFe]-hydrogenases in the archaeon *Methanococcus voltae* involves positive and negative control elements. *Genetics*, **52**, 1335–1341.